

Dalton Transactions

Accepted Manuscript



This is an *Accepted Manuscript*, which has been through the Royal Society of Chemistry peer review process and has been accepted for publication.

Accepted Manuscripts are published online shortly after acceptance, before technical editing, formatting and proof reading. Using this free service, authors can make their results available to the community, in citable form, before we publish the edited article. We will replace this *Accepted Manuscript* with the edited and formatted *Advance Article* as soon as it is available.

You can find more information about *Accepted Manuscripts* in the [Information for Authors](#).

Please note that technical editing may introduce minor changes to the text and/or graphics, which may alter content. The journal's standard [Terms & Conditions](#) and the [Ethical guidelines](#) still apply. In no event shall the Royal Society of Chemistry be held responsible for any errors or omissions in this *Accepted Manuscript* or any consequences arising from the use of any information it contains.

ARTICLE

Cite this: DOI: 10.1039/x0xx00000x

Received 00th January 2012,

Accepted 00th January 2012

DOI: 10.1039/x0xx00000x

www.rsc.org/

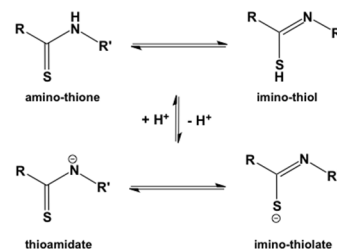
Deprotonation/Protonation-Driven Change of the σ -Donor Ability of a Sulfur Atom in Iron(II) Complexes with a Thioamide SNS Pincer Type Ligand

Tatsuya Suzuki,¹ Yuji Kajita² and Hideki Masuda^{1*}

A new iron complex with a thioamide SNS pincer type ligand, $[\text{FeBr}_2(\kappa^3\text{-H}_2\text{L}^{\text{DPM}})]$ ($\kappa^3\text{-H}_2\text{L}^{\text{DPM}} = 2,6\text{-bis}(N\text{-}2,6\text{-bis}(\text{diphenylmethyl})\text{-}4\text{-isopropylphenylthioamide})\text{pyridine}$) was synthesized. This complex reacts with NaH in THF to yield a unique Fe(II) complex with two THF molecules, $[\text{Fe}(\text{THF})_2(\kappa^3\text{-L}^{\text{DPM}})]$ ($\kappa^3\text{-L}^{\text{DPM}} = 2,6\text{-bis}(N\text{-}2,6\text{-bis}(\text{diphenylmethyl})\text{-}4\text{-isopropylphenyliminothiolate})\text{pyridine}$). The THF molecules of $[\text{Fe}(\text{THF})_2(\kappa^3\text{-L}^{\text{DPM}})]$ can be substituted with CO and CN-xylyl to give $[\text{Fe}(\text{CO})_3(\kappa^3\text{-L}^{\text{DPM}})]$ and $[\text{Fe}(\text{CN-xylyl})_3(\kappa^3\text{-L}^{\text{DPM}})]$, respectively. The complex $[\text{Fe}(\text{CN-xylyl})_3(\kappa^3\text{-L}^{\text{DPM}})]$ reacts with HBF_4 to produce $[\text{Fe}(\text{CN-xylyl})_3(\kappa^3\text{-H}_2\text{L}^{\text{DPM}})]^{2+}$ with protonated thioamide units. The difference in the IR spectra before and after protonation indicates that the major binding mode of CN-xylyl to iron(II) changes from π -back donation from metal to isocyanide to σ -donation from isocyanide to iron(II). This indicates that the σ -donor ability of the thioamide sulfur atom is tuned by deprotonation/protonation of thioamide.

Introduction

In recent years, the coordination chemistry of “pincer-type” tridentate ligands with metal ions has attracted significant attention from investigators in the fields of catalytic chemistry and material sciences.¹ In particular, the iron and cobalt complexes with bis-iminopyridine ligands (PDI), have been shown to have unique properties including elevated levels of catalytic activity for reactions such as olefin polymerization and dinitrogen activation, among others.² The thioamide pincer ligand has also been investigated. For example, Bowman-James and co-workers and Kanbara *et al.* each reported that Pd and Pt complexes with thioamide-based pincer ligands, which form a square planar structure, respectively, exhibit catalytic activities and photoluminescent properties.³ The thioamide group undergoes tautomerization between its amino-thione and imino-thiol forms, as shown in Scheme 1, and exhibits a stronger Brønsted acidity than the corresponding amide group. Consequently, when secondary thioamides are used as ligands, they are deprotonated (in the thionate form). This provides the ability to tune the electron density of the metal center by deprotonation/protonation. Kanbara *et al.* also reported that Ru(II) complexes with a thioamide pincer ligand can regulate the electronic properties of the metal center by deprotonation/protonation reactions of the NH groups on the secondary thioamide units.⁴ However, there have been no reports of an iron complex with a thioamide pincer ligand. In the case of other metal complexes, the Co complex with the thioamide pincer ligand formed a bischelate compound with an octahedral structure.⁵ In addition, the iron complexes with thiourea



Scheme 1. Equilibrium of secondary thioamide group

ARTICLE

tridentate ligands and an amide pincer ligand, which are similar to thioamide pincer ligand, formed bischelate compounds.^{6, 7} These bischelate compounds are not expected to have catalytic activity, because they have a tight structure and are difficult to exchange with other substituent ligands. We therefore designed and prepared a unique monochelate iron(II) complex with the thioamide pincer ligand. Here, we report the synthesis, structure, spectroscopic properties and an investigation of the reactivity of the new iron(II) complexes with the thioamide pincer ligand. Additionally, as an example, we examined the coordination behavior of the isocyanide molecule in deprotonation/protonation reactions of the NH groups on the thioamide units.

Results and Discussion

Preparations of H_2L^{DPM} ligand and its iron(II) complex

The ligand 2,6-bis(*N*-2,6-diphenylmethyl-4-isopropylphenylthioamide)pyridine (H_2L^{DPM}) was prepared according to a previously published method with slight modifications, where H_2L^{DPM} is an SNS pincer-type ligand with two bulky *N*-2,6-diphenylmethyl-4-isopropylphenylthioamide groups at the 2- and 6-positions of the pyridine unit. This ligand is expected to prevent the formation of a bischelate metal complex. The ligand was recrystallized from methanol to obtain a single crystal suitable for X-ray analysis. The molecular structure of H_2L^{DPM} is shown in Figure 1. The C=S bond lengths for H_2L^{DPM} are 1.648(2) and 1.651(2) Å and the C–N bond lengths are 1.340(3) and 1.339(3) Å, indicating that this ligand has a thioamide type structure (HN–(C=S)–) with a proton on each nitrogen atom.

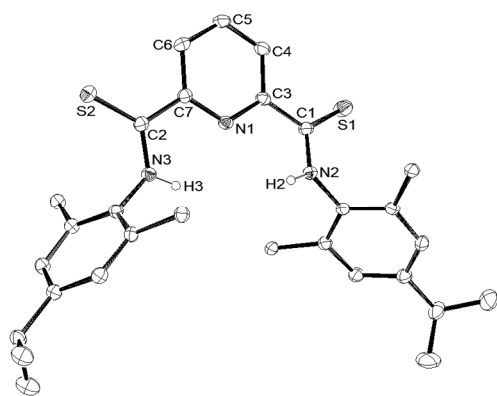


Figure 1. ORTEP view of the molecular structure of H_2L^{DPM} with ellipsoids at the 50% probability level. The hydrogen atoms and aromatic substituents on *N*-phenyl unit have been omitted for clarity except for H(2) and H(3). Selected bond lengths (Å) and angles (deg): C(1)–N(2) 1.340(3), C(2)–N(3) 1.339(3), C(1)–S(1) 1.648(2), C(2)–S(2) 1.651(2), S(1)–C(1)–N(2) 123.93(16), S(1)–C(1)–C(3)

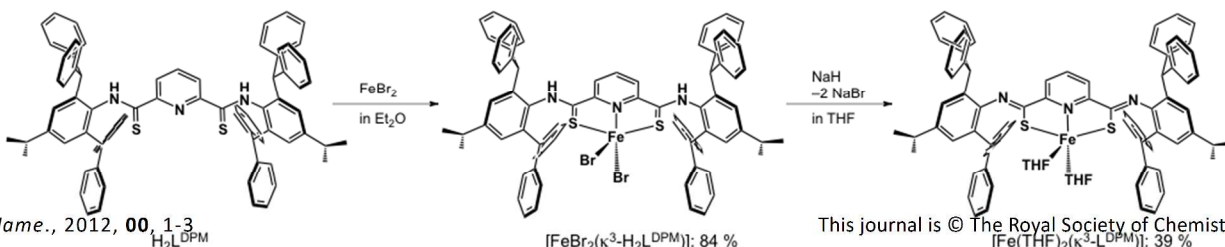
		Journal Name	
121.41(14),	N(2)–C(1)–C(3)	114.67(17),	S(2)–C(2)–N(3)
124.74(14),	S(2)–C(2)–C(7)	121.85(14),	N(3)–C(2)–C(7)
113.41(16).			

Treatment of H_2L^{DPM} with $FeBr_2$ in Et_2O under an argon atmosphere at room temperature produced a dark green solution after 24 h. A single crystal of $[FeBr_2(\kappa^3-H_2L^{DPM})]$ was obtained by slow evaporation from dimethoxyethane solution. The crystal structure of $[FeBr_2(\kappa^3-H_2L^{DPM})]$ is shown in Figure 2. The coordination geometry around the metal center for $[FeBr_2(\kappa^3-H_2L^{DPM})]$ is a distorted trigonal bipyramidal structure ($\tau = 0.60$);⁸ the bond angles Br(1)–Fe–Br(2) 123.19(5), Br(1)–Fe–N(1) 112.16(10) and Br(2)–Fe–N(1) 124.61(10) reveal that Br(1)–Br(2)–N(1) forms a trigonal plane and the angle S(1)–Fe–S(2) 160.93(6)° indicates that the arrangement of atoms S(1)–Fe–S(2) is essentially linear. The Fe–N(1) bond length for $[FeBr_2(\kappa^3-H_2L^{DPM})]$ is 2.164(4) Å, and the Fe–S(1) and Fe–S(2) bond lengths are 2.459(2) and 2.458(2) Å respectively. These Fe–N and Fe–S bond lengths are typical of those of a high-spin iron(II) complex as reported previously.⁹

This geometry is similar to that of the bis(iminopyridine)iron(II) complex $[FeBr_2(PDI)]$ reported previously.¹⁰ As the series of bis(imino)pyridine ligand, the iron complexes with PDI containing thioether have previously been reported, which is coordinated with N,N,N atoms to iron ion.¹¹ However, we could isolate only the iron complex coordinated with S,N,S atoms. This is the first report of a monochelate iron(II) complex with a thioamide pincer-type ligand, although there have been many reports on syntheses of iron(II) and cobalt(II) complexes with thiourea coordinated ligands in the *mer* configuration (each of these is octahedral bischelate metal complexes).^{5,7}

The C=S bond lengths of thioamide units for $[FeBr_2(\kappa^3-H_2L^{DPM})]$ are 1.649(4) and 1.667(5) Å and the C–N bond lengths are 1.326(7) and 1.323(7) Å, respectively. The former bond lengths are slightly longer than those of the metal-free ligand (1.648(2), 1.651(2) Å), and the latter bond lengths are shorter than those of the metal-free ligand (1.340(3), 1.339(3) Å). These findings indicate that the ligand is in the thioamide form (HN–(C=S)–) with a proton on each nitrogen atom.

The ¹H-NMR spectrum of $[FeBr_2(\kappa^3-H_2L^{DPM})]$ in THF-*d*₈ exhibited broadened peaks, indicating that the iron(II) complex is in the high-spin form. The $[FeBr_2(\kappa^3-H_2L^{DPM})]$ complex decomposed in MeOH, resulting in a yellow precipitate of H_2L^{DPM} . The solid-state magnetic moment of $[FeBr_2(\kappa^3-H_2L^{DPM})]$ was determined by the Evans method (using a magnetic susceptibility balance) to be 5.4 μ_B at 23 °C, which is consistent with the presence of four unpaired electrons. This finding has also been reported for the bis(imino)pyridine iron(II) complex, $[FeBr_2(PDI)]$.¹²

Preparation of $[Fe(THF)_2(\kappa^3-L^{DPM})]$ 

2 | *J. Name.*, 2012, 00, 1–3
 H_2L^{DPM}

Scheme 2. Synthesis of compounds $[FeBr_2(\kappa^3-H_2L^{DPM})]$ and $[Fe(THF)_2(\kappa^3-L^{DPM})]$.

This journal is © The Royal Society of Chemistry 2012
 $[Fe(THF)_2(\kappa^3-L^{DPM})]$: 39%

Journal Name

Stirring of $[\text{FeBr}_2(\kappa^3\text{-H}_2\text{L}^{\text{DPM}})]$ with excess NaH in THF solution under a dinitrogen atmosphere produces the bis-THF iron(II) compound $[\text{Fe}(\text{THF})_2(\kappa^3\text{-L}^{\text{DPM}})]$ (Scheme 2), which is also air- and moisture-sensitive. A single crystal of $[\text{Fe}(\text{THF})_2(\kappa^3\text{-L}^{\text{DPM}})]$ suitable for X-ray analysis was obtained from THF solution. The crystal structure of $[\text{Fe}(\text{THF})_2(\kappa^3\text{-L}^{\text{DPM}})]$ is shown in Figure 3. The coordination geometry of $[\text{Fe}(\text{THF})_2(\kappa^3\text{-L}^{\text{DPM}})]$ is square pyramidal ($\tau = 0.16$) with one pyridine nitrogen atom, N(1), two sulfur atoms, S(1) and S(2), and one THF oxygen atom, O(1), in the equatorial plane and one THF oxygen atom, O(2), in the axial position. This Fe(II) complex with THF molecules is available for substitution reaction.¹³

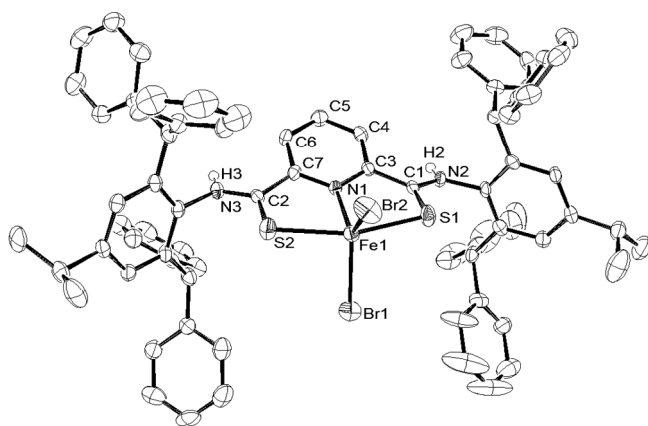


Figure 2. ORTEP view of the molecular structure of $[\text{Fe}(\kappa^3\text{-H}_2\text{L}^{\text{DPM}})\text{Br}_2]$ with ellipsoids at the 50% probability level. The hydrogen atoms have been omitted for clarity except for H(2) and H(3). Selected bond lengths (Å) and angles (deg): Br(1)–Fe(1) 2.4272(12), Br(2)–Fe(1) 2.4642(12), Fe(1)–S(1) 2.459(2), Fe(1)–S(2) 2.458(2), Fe(1)–N(1) 2.164(4), S(1)–C(1) 1.674(5), S(2)–C(2) 1.667(5), N(2)–C(1) 1.326(7), N(3)–C(2) 1.323(7), Br(1)–Fe(1)–Br(2) 123.19(5), Br(1)–Fe(1)–N(1) 112.16(10), Br(2)–Fe(1)–N(1) 124.61(10), S(1)–Fe(1)–S(2) 160.93(6).

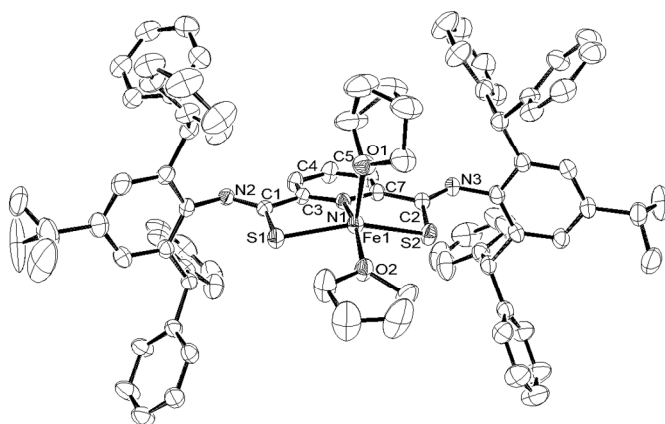


Figure 3. ORTEP view of the molecular structure of $[\text{Fe}(\text{THF})_2(\kappa^3\text{-L}^{\text{DPM}})]$ with ellipsoids at the 50% probability level. The hydrogen atoms have been omitted for clarity. Selected bond lengths (Å),

angles (deg): Fe(1)–S(1) 2.3600(8), Fe(1)–S(2) 2.3621(8), Fe(1)–O(1) 2.0639(19), Fe(1)–O(2) 2.1418(18), Fe(1)–N(1) 2.1593(19), S(1)–C(1) 1.744(3), S(2)–C(2) 1.758(3), N(2)–C(1) 1.286(4), N(3)–C(2) 1.284(3), S(1)–Fe(1)–S(2) 151.30(3), O(2)–Fe(1)–N(1) 162.05(8).

Such a combination does not typically form a stable complex.¹⁴ The C–S bond lengths of $[\text{Fe}(\text{THF})_2(\kappa^3\text{-L}^{\text{DPM}})]$ are 1.744(3) and 1.758(3) Å and the C–N bond lengths are 1.286(4) and 1.284(3) Å. The C–S bond lengths are longer and the C=N bond lengths are shorter in comparison with those of the $[\text{FeBr}_2(\kappa^3\text{-H}_2\text{L}^{\text{DPM}})]$ complex described above. These observations are explained in terms of a structural change involving deprotonation of the NH groups on the secondary thioamide unit to form imino-thiolate. The deprotonation of NH groups was confirmed in a comparison of IR spectra of $[\text{FeBr}_2(\kappa^3\text{-H}_2\text{L}^{\text{DPM}})]$ and $[\text{Fe}(\text{THF})_2(\kappa^3\text{-L}^{\text{DPM}})]$. The NH stretching vibration bands of $[\text{FeBr}_2(\kappa^3\text{-H}_2\text{L}^{\text{DPM}})]$ were found at 3327 cm^{-1} and at 3157 cm^{-1} , while the analogous bands in $[\text{Fe}(\text{THF})_2(\kappa^3\text{-L}^{\text{DPM}})]$ disappeared upon reaction with NaH. The formation of the imino-thiolate is indicated by the metal-to-ligand bond lengths. The lengths of Fe–N(1) (2.1593(19)), Fe–S(1) (2.3600(8)), and Fe–S(2) (2.3621(8)) bonds for $[\text{Fe}(\text{THF})_2(\kappa^3\text{-L}^{\text{DPM}})]$ are each shortened upon deprotonation. This indicates that the σ -donation of the imino-thiolate ligand is strengthened relative to the bond strength of the protonated thioamide form. This complex is paramagnetic, as determined by its $^1\text{H-NMR}$ spectrum in THF- d_8 . The solid-state magnetic moment of $[\text{Fe}(\text{THF})_2(\kappa^3\text{-L}^{\text{DPM}})]$ was determined by magnetic susceptibility measurements to be 5.2 μ_B at 23 °C, which is consistent with that of an iron(II) complex with four unpaired electrons.

Reaction of $[\text{Fe}(\text{THF})_2(\kappa^3\text{-L}^{\text{DPM}})]$ with CO.

The red precipitate of $[\text{Fe}(\text{THF})_2(\kappa^3\text{-L}^{\text{DPM}})]$ reacted with CO in toluene, and the resulting orange solution was stored at -30 °C (Scheme 3). The resultant complex $[\text{Fe}(\text{CO})_3(\kappa^3\text{-L}^{\text{DPM}})]$ was in the form of a yellow crystalline solid (precipitated from toluene solution), and was characterized by $^1\text{H-NMR}$ and $^{13}\text{C-NMR}$ spectrometry, infrared spectroscopy and elemental analyses. The complex $[\text{Fe}(\text{CO})_3(\kappa^3\text{-L}^{\text{DPM}})]$ is diamagnetic, and its $^1\text{H-NMR}$ spectrum displays resonances in the diamagnetic range. In $^{13}\text{C-NMR}$, the carbon atoms of the coordinated CO ligands were clearly observed at 206.9 and 200.3 ppm with an integration ratio of 1:2 and the thioamide carbon atoms were observed at 169.5 ppm. Fortunately, we obtained a single crystal of complex $[\text{Fe}(\text{CO})_3(\kappa^3\text{-L}^{\text{DPM}})]$, and the X-ray analysis revealed that the iron ion is engaged by the thioamide pincer-type ligand and three carbonyl ligands (Figure 4). The coordination geometry is distorted octahedral with the SNS pincer type ligand (Fe–N(1) 1.980(2), Fe–S(1) 2.2676(11), Fe–S(2) 2.2638(11)), in which one coordinated CO molecule (Fe–C(4) 1.791(3)) is positioned within the pincer plane, and two CO molecules (Fe–C(3) 1.861(3) and Fe–C(5) 1.825(3)) are located in *trans* positions each other. The Fe–S(1) and Fe–S(2) bonds are shorter than those of $[\text{Fe}(\text{CN-xylyl})_3(\kappa^3\text{-L}^{\text{DPM}})]$ as describe below and the Fe–CO bond in the pincer plane is significantly shorter than the other two Fe–CO bonds, indicating that the Fe–CO bond in the

ARTICLE

pincer plane is shortened by the trans influence of the thioamide ligand. On the other hand, the Fe–CO bonds of the other two carbonyls are elongated by trans influence through the π -back donation from metal to CO ligand. Further support for trans influence is provided by ^{13}C -NMR data; the carbonyl carbon atom in the pincer plane is observed in the lower magnetic field region relative to the two carbonyl carbon atoms at the trans positions, although it was not significantly affected to their C–O bond lengths. In the IR spectrum of $[\text{Fe}(\text{CO})_3(\kappa^3\text{-L}^{\text{DPM}})]$, two vibrations were detected as the coordinated CO stretching bands. From the above findings, the 2044 cm^{-1} band was tentatively assigned as that of the two carbonyls located at the trans positions and the 1993 cm^{-1} as a carbonyl in the pincer plane.

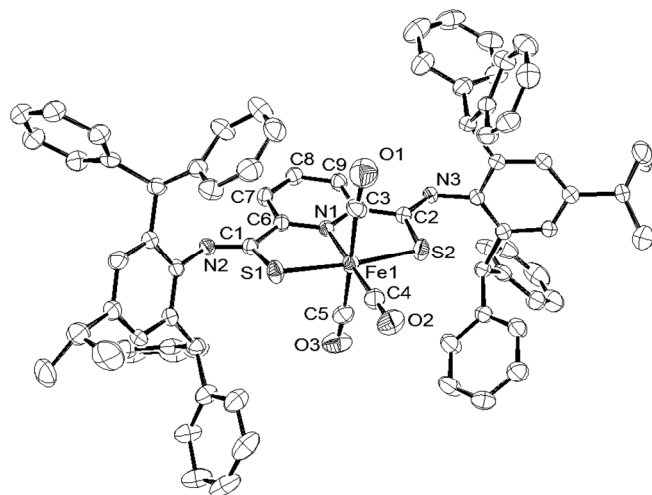
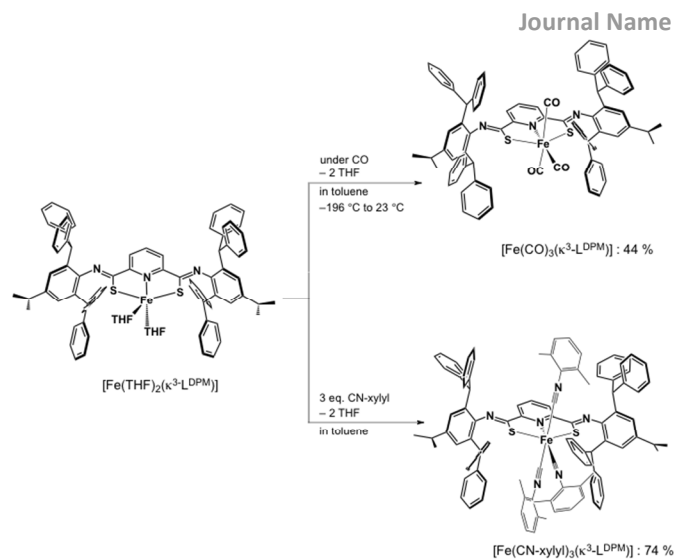


Figure 4. ORTEP view of the molecular structure of $[\text{Fe}(\text{CO})_3(\kappa^3\text{-L}^{\text{DPM}})]$ with ellipsoids at the 50% probability level. The hydrogen atoms have been omitted for clarity. Selected bond lengths (Å): Fe(1)–S(1) 2.2676(11), Fe(1)–S(2) 2.2638(11), Fe(1)–N(1) 1.980(2), Fe(1)–C(3) 1.861(3), Fe(1)–C(4) 1.791(3), Fe(1)–C(5) 1.825(3), S(1)–C(1) 1.743(3), S(2)–C(2) 1.745(3), N(2)–C(1) 1.291(3), N(3)–C(2) 1.285(4), S(1)–Fe(1)–S(2) 173.39(3), S(1)–Fe(1)–N(1) 86.73(7), S(1)–Fe(1)–C(3) 90.51(11), S(1)–Fe(1)–C(4) 93.98(11), S(1)–Fe(1)–C(5) 89.49(12), S(2)–Fe(1)–N(1) 87.05(8), S(2)–Fe(1)–C(3) 87.04(11), S(2)–Fe(1)–C(4) 92.25(11), S(2)–Fe(1)–C(5) 92.41(12), N(1)–Fe(1)–C(3) 87.88(10), N(1)–Fe(1)–C(5) 86.99(10), C(3)–Fe(1)–C(4) 92.30(12), C(4)–Fe(1)–C(5) 92.82(12).



Scheme 3. Synthesis of compounds $[\text{Fe}(\text{CO})_3(\kappa^3\text{-L}^{\text{DPM}})]$ and $[\text{Fe}(\text{CN-xylyl})_3(\kappa^3\text{-L}^{\text{DPM}})]$.

Reaction of $[\text{Fe}(\text{THF})_2(\kappa^3\text{-L}^{\text{DPM}})]$ with 2,6-dimethylbenzene isocyanide (CN-xylyl)

The reaction of $[\text{Fe}(\text{THF})_2(\kappa^3\text{-L}^{\text{DPM}})]$ with 3 equiv of CN-xylyl in toluene afforded $[\text{Fe}(\text{CN-xylyl})_3(\kappa^3\text{-L}^{\text{DPM}})]$ as a red crystal (Scheme 3) which was characterized by ^1H -NMR and ^{13}C -NMR spectrometry, infrared spectroscopy and elemental analysis. The ^1H -NMR spectrum of the complex displays resonances in the normal magnetic field region, indicating that the complex is in the low-spin state. The methyl protons of the xylyl group were clearly observed at 2.268 and 1.878 ppm with a 1:2 integral ratio, although certain peaks assignable to aromatic protons observed in the 6.7 – 7.2 ppm region are less informative due to overlapping of peaks. The compound $[\text{Fe}(\text{CN-xylyl})_3(\kappa^3\text{-L}^{\text{DPM}})]$ was stable under air and in the presence of moisture. Fortunately, we obtained a single crystal suitable for X-ray analysis. The crystal structure analysis, as shown in Figure 5, clearly revealed that the complex $[\text{Fe}(\text{CN-xylyl})_3(\kappa^3\text{-L}^{\text{DPM}})]$ has a distorted octahedral structure with an SNS pincer-type ligand, one isocyanide carbon atom in the pincer plane and two isocyanide carbon atoms located at trans positions each other. The lengths of Fe–N(1), Fe–S(1), Fe–S(2), and Fe–C(79) bonds in the pincer plane are 1.9844(17), 2.2807(10), 2.2744(10), and 1.809(3) Å, respectively, and the Fe–C(79) bond length is shorter than the Fe–C(78) (1.871(4) Å) and Fe–C(80) (1.874(4) Å) bonds. The lengths of the two C–S bonds are 1.743(3) and 1.739(2) Å, and those of two C–N bond are 1.288(4) and 1.286(3) Å, respectively. These bond lengths are almost the same as those of $[\text{Fe}(\text{CO})_3(\kappa^3\text{-L}^{\text{DPM}})]$ and $[\text{Fe}(\text{THF})_2(\kappa^3\text{-L}^{\text{DPM}})]$ with the imino-thiolate ligand in spite of the difference in their spin states (the former is low-spin and the latter is high-spin). However, the C–S and C–N bonds for $[\text{Fe}(\text{CN-xylyl})_3(\kappa^3\text{-L}^{\text{DPM}})]$ are clearly elongated and shortened, respectively in comparison with those of $[\text{FeBr}_2(\kappa^3\text{-H}_2\text{L}^{\text{DPM}})]$ with the thioamide ligand described above.

Journal Name

Next, $[\text{Fe}(\text{CN-xylyl})_3(\kappa^3\text{-L}^{\text{DPM}})]$ was mixed with 2 equiv of HBF_4 in toluene. A brown precipitate of $[\text{Fe}(\text{CN-xylyl})_3(\kappa^3\text{-H}_2\text{L}^{\text{DPM}})] \cdot 2(\text{BF}_4)$ was obtained in which the two imino-thiolate nitrogen atoms were protonated. The $^1\text{H-NMR}$ spectrum of the precipitate in CDCl_3 solution has an NH proton peak at 10.51 ppm, indicating that the imino-thiolate nitrogen of the compound is protonated to afford $[\text{Fe}(\text{CN-xylyl})_3(\kappa^3\text{-H}_2\text{L}^{\text{DPM}})]^{2+}$. Such a phenomenon was not observed when a weaker acid such as trimethylammonium chloride and 2,6-lutidinium tetrafluoroborate was added. Further evidence of protonation was provided by a comparison of IR spectra of $[\text{Fe}(\text{CN-xylyl})_3(\kappa^3\text{-L}^{\text{DPM}})]$ and $[\text{Fe}(\text{CN-xylyl})_3(\kappa^3\text{-H}_2\text{L}^{\text{DPM}})] \cdot 2(\text{BF}_4)$; the NH stretching vibration band for $[\text{Fe}(\text{CN-xylyl})_3(\kappa^3\text{-H}_2\text{L}^{\text{DPM}})] \cdot 2(\text{BF}_4)$ appeared at 3266 cm^{-1} upon addition of HBF_4 to $[\text{Fe}(\text{CN-xylyl})_3(\kappa^3\text{-L}^{\text{DPM}})]$, indicating that the imino-thiolate groups are converted to thioamides. Furthermore, the band representing the stretching vibration of the coordinated isocyanide units $\nu(\text{C}\equiv\text{N})$ was shifted from 2110 cm^{-1} to 2144 cm^{-1} upon protonation of the imino-thiolate units. This stretching vibration is significantly higher than that of metal free CN-xylyl molecule (2121 cm^{-1}), which indicates that the σ -donation from the sulfur atoms to the metal ion is weakened with the conversion from imino-thiolate to thioamide groups. We think this finding as follows. The π -back donation from the metal ion to the π^* orbitals of isocyanide ligands are reduced and the σ -donation from the σ^* orbital of isocyanide carbon to metal ion increases.

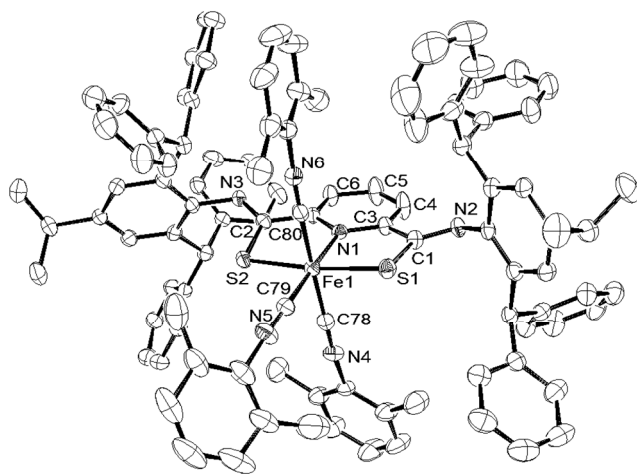


Figure 5. ORTEP view of the molecular structure of $[\text{Fe}(\text{CN-xylyl})_3(\kappa^3\text{-L}^{\text{DPM}})]$ with ellipsoids at the 50 % probability level. The hydrogen atoms have been omitted for clarity. Selected bond lengths (\AA) and angles (deg): Fe(1)–S(1) 2.2807(10), Fe(1)–S(2) 2.2744(10), Fe(1)–N(1) 1.9844(17), Fe(1)–C(78) 1.871(4), Fe(1)–C(79) 1.809(3), Fe(1)–C(80) 1.874(4), S(1)–C(1) 1.743(3), S(2)–C(2) 1.739(2), N(2)–C(1) 1.288(4), N(3)–C(2) 1.286(3), S(1)–Fe(1)–S(2) 172.33(3), S(1)–Fe(1)–N(1) 86.49(8), S(1)–Fe(1)–C(78) 90.39(10), S(1)–Fe(1)–C(79) 95.04(11), S(1)–Fe(1)–C(80) 90.24(10), S(2)–Fe(1)–N(1) 86.00(7), S(2)–Fe(1)–C(78) 91.13(10), S(2)–Fe(1)–C(79) 92.45(11), S(2)–Fe(1)–C(80) 87.90 (10), N(1)–Fe(1)–C(78) 89.49(10), N(1)–Fe(1)–C(80) 87.90(10), C(78)–Fe(1)–C(79) 91.17(13), C(79)–Fe(1)–C(80) 91.41(13).

Conclusion

In order to examine the binding behavior of the thioamide pincer type ligand toward the metal and effects relating to deprotonation/protonation of its thioamide group, we synthesized a new monochelate iron(II) complex, $[\text{FeBr}_2(\kappa^3\text{-H}_2\text{L}^{\text{DPM}})]$, with a thioamide SNS pincer type ligand which includes a bulky substituent group, $\kappa^3\text{-H}_2\text{L}^{\text{DPM}}$. The complex was characterized and ligand substitution reactions were investigated. To the best of our knowledge, this is the first report of a monochelate iron(II) complex with a thioamide pincer-type ligand. The two bromide ions of the iron complex were substituted with THF molecules in THF solution. The THF ligands of the $[\text{Fe}(\text{THF})_2(\kappa^3\text{-L}^{\text{DPM}})]$ complex were easily substituted with CO and CN-xylyl molecules to give $[\text{Fe}(\text{CO})_3(\kappa^3\text{-L}^{\text{DPM}})]$ and $[\text{Fe}(\text{CN-xylyl})_3(\kappa^3\text{-L}^{\text{DPM}})]$, respectively. These complexes each had a distorted octahedral structure in a low spin state. The imino-thiolate units of the $[\text{Fe}(\text{CN-xylyl})_3(\kappa^3\text{-L}^{\text{DPM}})]$ complex can be protonated to thioamide units to give $[\text{Fe}(\text{CN-xylyl})_3(\kappa^3\text{-H}_2\text{L}^{\text{DPM}})] \cdot 2(\text{BF}_4)$. The band representing the CN stretching vibration of the coordinated CN group of $[\text{Fe}(\text{CN-xylyl})_3(\kappa^3\text{-L}^{\text{DPM}})]$ was shifted by 34 cm^{-1} to a higher energy region upon protonation. The above findings may be explained in terms of the σ and π bonding characters between metal and ligands as follows; the σ -donation from the sulfur atoms to the iron ion is weakened by conversion from imino-thiolate to thioamide, which made the π -back donation from the metal ion to isocyanide reduced and made the σ -donation from the isocyanide carbon to the metal ion increased. These suggest that they are controlled by the process of deprotonation/protonation.

Experimental

Materials.

All of the reagents and solvents employed are commercially available. All anhydrous solvents were purchased from Wako Ltd., and were degassed with argon. 2,6-pyridinedicarbonyl dichloride was synthesized according to the previously published method.¹⁴

General Methods.

All manipulations were carried out under an atmosphere of purified argon or dinitrogen gas in an mBRAUN MB 150B-G glovebox or by standard Schlenk techniques. $^1\text{H-NMR}$ and $^{13}\text{C-NMR}$ spectra were measured on a Varian Mercury 300 spectrometer, and ^1H chemical shifts were estimated relative to TMS as an internal standard. Fourier transform infrared (FT-IR) spectra of solid compounds were measured as KBr pellets using a JASCO FT/IR-410 spectrophotometer. Elemental analyses were obtained with a Perkin-Elmer CHN-900 elemental analyzer. Magnetic moment measurements (Evans method) in the solid state were obtained using a Sherwood Scientific Ltd. MSB-MKI magnetic susceptibility balance.

ARTICLE

Journal Name

X-ray crystallography. Each crystal was mounted on a glass fiber and diffraction data were collected using a Rigaku/MSC Mercury CCD with graphite monochromated Mo-K α radiation at -100 °C or -150 °C. Crystal data and experimental details are listed in Table S1 (Supporting Information). The crystal structures of all Fe(II) complexes were solved by a combination of direct methods (SIR92¹⁶ or SIR2004¹⁷) and Fourier techniques. All non-hydrogen atoms were refined anisotropically. Hydrogen atoms were refined by the riding model using the appropriate HFIX command in SHELXL97.¹⁸ The Sheldrick weighting scheme was applied. Plots of $\Sigma(|F_o| - |F_c|)^2$ versus $|F_o|$, reflection order in data collection, $\sin \theta/\lambda$, and various classes of indices showed no unusual trends. Neutral atomic scattering factors were taken from International Tables for X-ray Crystallography edited by Cromer and Waber.¹⁹ Anomalous dispersion effects were included in F_{calc} ,²⁰ where the values for $\Delta f'$ and $\Delta f''$ were taken from those of Creagh and McAuley.²¹ The values for the mass attenuation coefficients are those of Creagh and Hubbell.²² All calculations were performed using the crystallographic software package, CrystalStructure.

Syntheses of compounds**2,6-Bis(diphenylmethyl)-4-isopropylaniline**

The compound was prepared by according to the method described by Markó *et al.*²³ Diphenylmethanol (10.0 g 0.0542 mol), HCl (36 % HCl, 2 mL), ZnCl₂ (2.00 g, 0.0146 mol), and 4-isopropylaniline (3.66 g 0.0271 mol) were added to a 100 mL Schlenk tube. The mixture was heated at 160 °C to melt the diphenylmethanol. Once cooled, the solid was dissolved in CH₂Cl₂ and washed successively with NaHCO₃. After drying over Na₂SO₄, the mixture was filtered. Evaporation of the solvent *in vacuo* yielded an off-white solid, which was washed with *n*-hexane to give 2,6-bis(diphenylmethyl)-4-isopropylaniline as a white powder (9.66 g, yield: 76 %). ¹H-NMR (δ /ppm vs TMS in CDCl₃, 300 MHz): 7.27 (t, 8H, CH_{Ph}), 7.21 (t, 4H, CH_{Ph}), 7.08 (d, 8H, CH_{Ph}), 6.42 (s, 2H, CH_{Ph}), 5.45 (s, 2H, CH(Ph)₂), 3.26 (s, 2H, NH₂), 2.55 (m, 1H, CH(CH₃)₂), 0.93 (d, 6H, CH₃).

2,6-Bis(N-2,6-bis(diphenylmethyl)-4-isopropylphenylamide)pyridine

2,6-Pyridinedicarboxylic dichloride (5.00 g 10.6×10^{-3} mol) was dissolved in 100 mL of dry THF. To this solution was added 2,6-bis(diphenylmethyl)-4-isopropylaniline (1.09 g 5.34×10^{-3} mol) and triethylamine (1.50 mL 0.0106 mol) at 0 °C. The mixture was stirred at room temperature overnight. The precipitate of Et₃N·HCl was filtered and the solvent was removed under vacuum, dissolved in CHCl₃ and purified by silica gel column chromatography. 2,6-bis(N-2,6-bis(diphenylmethyl)-4-isopropylphenylamide)pyridine was isolated as white powder (yield: 3.51 g 62 %). ¹H-NMR (δ /ppm vs TMS in CDCl₃, 300 MHz): 7.95 (t, 1H, CH_{py}), 8.27 (d, 2H, CH_{py}), 7.98 (s, 2H, NH), 5.43 (s, 4H, CH(Ph)₂), 6.87 (br, 16H, CH_{Ph}), 6.87 (br, 16H, CH_{Ph}), 6.87 (br, 8H, CH_{Ph}), 6.73 (s, 4H, CH_{Ph}), 2.72 (m,

2H, CH(CH₃)₂), 1.05 (d, 12H, CH₃). ESI TOF MS: m/z 1088.7 [M + Na]⁺, 1066.7 [M + H]⁺. FTIR (KBr, cm⁻¹): 3371(NH), 1687 (C=O).

2,6-Bis(N-2,6-bis(diphenylmethyl)-4-isopropylphenylthioamide)pyridine (H₂L^{DPM})

Lawesson's reagent (3.79 g, 9.33×10^{-3} mol) was added to a solution of 2,6-bis(N-2,6-bis(diphenylmethyl)-4-isopropylphenylamide)pyridine (5 g 4.69×10^{-3} mol) in toluene (30 mL), and the mixture was heated at 100 °C for 6 h. After cooling, the precipitate was filtered and the solvent was removed under vacuum. The precipitate was dissolved in CHCl₃ and purified by silica gel column chromatography. 2,6-Bis(N-2,6-bis(diphenylmethyl)-4-isopropylphenylthioamide)pyridine was isolated as yellow powder of H₂L^{DPM} ligand (2.53 g 49 %). ¹H-NMR (δ /ppm vs TMS in CDCl₃, 300 MHz): 8.02 (t, 1H, CH_{py}), 8.77 (d, 2H, CH_{py}), 9.42 (s, 2H, NH), 5.37 (s, 4H, CH(Ph)₂), 6.97 (d, 8H, CH_{Ph}), 6.64 (d, 8H, CH_{Ph}), 7.13 (t, 8H, CH_{Ph}), 6.56 (t, 8H, CH_{Ph}), 7.15 (t, 8H, CH_{Ph}), 6.41 (t, 8H, CH_{Ph}), 6.84 (s, 4H, CH_{Ph}), 2.78 (m, 2H, CH(CH₃)₂), 1.10 (d, 12H, CH₃). ESI TOF MS: m/z 1120.5 [M + Na]⁺, M = 1097.5 (C₇₇H₆₇N₃S₂). FTIR (KBr, cm⁻¹): 3301(NH), 994 (C=S). Anal. Calcd. for C₇₇H₆₇N₃S₂: C, 84.19; H, 6.15; N, 3.38; S, 5.84. Found: C 83.75; H 5.93; N 3.83; S, 5.52.

[FeBr₂(κ^3 -H₂L^{DPM})]

To a diethylether (3 mL) solution of H₂L^{DPM} (100 mg, 9.10×10^{-2} mmol) was added FeBr₂ (8.28 mg, 9.10×10^{-2} mmol), followed by stirring at room temperature. After 24 hours, the mixture was filtered and washed with diethylether to give a green powder. The powder was dissolved in CH₂Cl₂, and the precipitate was filtered. The solvent was removed under vacuum to yield a green precipitate of [FeBr₂(κ^3 -H₂L^{DPM})] (100.4 mg, 84 %). The complex was recrystallized from DME as dark green needle-like crystals. ESI TOF MS: m/z 1235.3 [M - Br]⁺, M = 1313.0 (C₇₇H₆₇N₃S₂FeBr₂). Anal. Calcd. for C₇₇H₆₇N₃S₂FeBr₂: C, 70.37; H, 5.14; N, 3.20; S, 4.88. Found: C, 70.09; H, 5.24; N, 2.98; S, 5.01.

[Fe(THF)₂(κ^3 -L^{DPM})]

To a THF (3 mL) solution of [FeBr₂(κ^3 -H₂L^{DPM})] (100 mg, 7.61×10^{-2} mmol) was added NaH (20 mg, 8.33×10^{-1} mmol) with stirring at room temperature. After 2 hours, the color of the reaction mixture changed from green to orange-red. The precipitate was filtered and the mixture was stored at -30 °C overnight, leading to formation of orange crystals of [Fe(THF)₂(κ^3 -L^{DPM})] (38 mg, 39 %).

FTIR(KBr, cm⁻¹): 3082, 3059, 3024, 2958, 2924, 2868 (CH₃), 1948, 1884, 1807, 1598 (C=C), 1565 (C=N). Anal. Calcd. for C₈₅H₇₉N₅S₂O₂Fe: C, 78.86; H, 6.15; N, 3.25; S, 4.95. Found: C, 77.53; H, 6.23; N, 3.18; S, 4.83.

[Fe(CO)₃(κ^3 -L^{DPM})]

A toluene (3 mL) solution of [Fe(THF)₂(κ^3 -L^{DPM})] (100 mg, 7.71×10^{-2} mmol) was placed under 1 atm of carbon monoxide at -196 °C. When the resulting reaction mixture was warmed to ambient temperature and stirred for 48 h, the solution color changed from orange to brownish yellow. After 48 hours, the solvent was removed

Journal Name

under vacuum, forming a dark brown powder of $[\text{Fe}(\text{CO})_3(\kappa^3\text{-L}^{\text{DPM}})]$. The brown powder was dissolved in toluene and stored at $-50\text{ }^\circ\text{C}$ for 24 hours, leading to formation of $[\text{Fe}(\text{CO})_3(\kappa^3\text{-L}^{\text{DPM}})]$ crystals (42 mg, 44 %). $^1\text{H-NMR}$ (δ/ppm from TMS in benzene- d_6 , 300 MHz): 7.71 (t, 1H, $\text{Py}_{(4)}$), 7.29-7.13 (overlapped with solvent peaks), 5.976 (s, 4H, $\text{CH}(\text{Ph})_2$), 2.508 (m, 2H, $\text{CH}(\text{Me})_2$), 0.970 (d, 12H, $\text{CH}(\text{CH}_3)_2$). $^{13}\text{C-NMR}$ (δ/ppm from solvent in CDCl_3): 206.9 (CO), 200.3 (CO), 169.5 (CS), 159.1, 145.6, 143.9, 143.8, 143.5, 132.3, 129.8, 129.3, 128.3, 128.1, 126.5, 126.2, 126.0, 125.9, 52.5 ($\text{CH}(\text{Ph})_2$), 33.6 ($\text{CH}(\text{CH}_3)_2$), 24.1 ($\text{CH}(\text{CH}_3)_2$). FTIR (KBr, cm^{-1}): 3082, 3059, 3024, 2958, 2924, 2868 (CH_3), 2044, 1993 (CO), 1948, 1884, 1807, 1598 (C=C), 1565 (C-N). Anal. Calcd. for $\text{C}_{80}\text{H}_{68}\text{N}_3\text{S}_2\text{FeO}_3$: C, 77.53; H, 5.53; N, 3.39, S, 5.17. Found: C, 77.85; H, 5.72 2.88; N 4.89; S, 4.82.

 $[\text{Fe}(\text{CN-xylyl})_3(\kappa^3\text{-L}^{\text{DPM}})]$

To a toluene (3 mL) solution of $[\text{Fe}(\text{THF})_2(\kappa^3\text{-L}^{\text{DPM}})]$ (100 mg, 7.71×10^{-2} mmol) was added 2,6-xylylisocyanide (30.4 mg, 2.32×10^{-1} mmol) with stirring at room temperature. After 6 hours, the mixture was stored at $-50\text{ }^\circ\text{C}$ overnight, leading to formation of red crystals of $[\text{Fe}(\text{CN-xylyl})_3(\kappa^3\text{-L}^{\text{DPM}})]$ (88 mg, 74 %).

$^1\text{H-NMR}$ (δ/ppm from TMS in benzene- d_6 , 300 MHz): 7.783 (d, 2H, $\text{Py}_{(3,5)}$), 7.419 (d, 8H, $\text{Ph}_{(2,6)}$), 6.714 (t, 1H, $\text{Py}_{(4)}$), 6.781 – 7.124 (m, 14H, Ph, Xylyl), 6.477 (m, 3H, Xylyl), 6.377 (d, 4H, Xylyl), 5.976 (s, 4H, $\text{CH}(\text{Ph})_2$), 2.508 (m, 2H, $\text{CH}(\text{Me})_2$), 2.268 (s, 6H, Xylyl), 1.878 (s, 12H, Xylyl), 0.970 (d, 12H, $\text{CH}(\text{CH}_3)_2$). $^{13}\text{C-NMR}$ (δ/ppm from solvent in CDCl_3): 175.18 (xylyl), 175.29 (xylyl), 160.79 (CS), 147.85, 145.21, 144.12, 142.12, 138.13, 135.61, 134.68, 134.47, 132.12, 130.05, 129.43, 129.31, 128.04, 128.50, 127.75, 127.66, 126.48, 125.59, 124.22, 51.97 (Ph_2CH), 33.63 ($\text{Ar-CH}(\text{CH}_3)_2$), 24.28 ($\text{Ar-CH}(\text{CH}_3)_2$), 19.45 (xylyl), 18.50 (xylyl). FTIR (KBr, cm^{-1}): 3082, 3059, 3024, 2953, 2922, 2854 (CH_3), 2110, 2087 (CN), 1948, 1884, 1807, 1598 (C=C), 1538 (C-N). Anal. Calcd. for $\text{C}_{104}\text{H}_{92}\text{N}_6\text{S}_2\text{Fe}$: C, 80.80; H, 6.00; N, 5.44; S, 4.15. Found: C, 79.67; H 6.04; N 5.16; S, 4.10.

 $[\text{Fe}(\text{CN-xylyl})_3(\kappa^3\text{-H}_2\text{L}^{\text{DPM}})](\text{BF}_4)_2$

To a toluene (3 mL) solution of $[\text{Fe}(\text{CN-xylyl})_3(\kappa^3\text{-L}^{\text{DPM}})]$ (100 mg, 7.71×10^{-2} mmol) was added HBF_4 (20 μL , 1.47×10^{-1} mmol) with stirring at room temperature. After 6 hours, the reaction mixture changed from a red solution to a brown slurry. The precipitate was collected on a funnel, washed with pentane and dried (79 mg, 60 %).

$^1\text{H-NMR}$ (δ/ppm from TMS in benzene- d_6 , 300 MHz): 10.51 (s, 2H, NH), 8.59 (t, 1H, $\text{Py}_{(4)}$), 8.16 (d, 2H, $\text{Py}_{(3,5)}$), 7.40-5.44 (overlapped with solvent peaks), 5.44 (s, 4H, Ar-CHPh_2), 2.69 (m, 2H, $\text{CH}(\text{CH}_3)_2$), 2.52 (s, 6H, Xylyl), 1.89 (s, 12H, xylyl), 0.99 (d, 12H, $\text{CH}(\text{CH}_3)_2$).

$^{13}\text{C-NMR}$ (δ/ppm vs solvent in CDCl_3): 194.71 (CS), 155.71 (xylyl), 150.57 (xylyl), 142.56, 142.16, 140.89, 134.88, 134.63, 131.77, 130.30, 130.17, 129.25, 129.06, 128.86, 128.73, 128.51, 128.44, 127.86, 127.58, 127.24, 126.54, 126.16, 52.03 (Ph_2CH), 33.91 ($\text{Ar-CH}(\text{CH}_3)_2$), 23.69 ($\text{Ar-CH}(\text{CH}_3)_2$), 19.38 (xylyl), 18.52 (xylyl).

FTIR (KBr, cm^{-1}): 3269 (NH), 3082, 3059, 3024, 2953, 2922, 2869 (CH_3), 22175, 2144 ($\text{C}\equiv\text{N}$), 1948, 1884, 1807, 1150, 1127, 1077,

1051 (BF_4). Anal. Calcd. for $\text{C}_{104}\text{H}_{94}\text{N}_6\text{S}_2\text{FeB}_2\text{F}_8$: C, 72.56; H, 5.50; N, 4.88; S, 3.73. Found: C, 71.86; H, 5.54; N, 4.50; S, 3.52.

Acknowledgements

We thank Professor M. D. Fryzuk (The University of British Columbia) for his helpful comments. We gratefully acknowledge for the support of this work by a Grant-in-Aid for Scientific Research from the Ministry of Education, Culture, Sports, Science and by Japan Society for the Promotion of Science "Strategic Young Researcher Overseas Visits Program for Accelerating Brain Circulation".

Notes and References

¹ Department of Frontier Materials, Graduate School of Engineering, Nagoya Institute of Technology, Gokiso, Showa, Nagoya 466-8555, Japan

² Department of Applied Chemistry, Aichi Institute of Technology, 1247 Yachigusa, Yakusa-cho, Toyota 470-0392, Japan

Fax: +81-52-735-5209; Tel: +81-52-735-5228;

E-mail: masuda.hideki@nitech.ac.jp

- V. C. Gibson, G. A. Solan, *Top. Organomet. Chem.*, **2009**, *26*, 107-158. V. C. Gibson, C. Redshaw, G. A. Solan, *Chem. Rev.*, **2007**, *107*, 1745-1776. C. Bianchini, G. Giambastiani, I. Guerrero Rios, G. Mantovani, A. Meli, A. M. Segarra, *Coord. Chem. Rev.*, **2006**, *250*, 1391-1418. B. L. Small, M. Brookhart, *Macromolecules* **1999**, *32*, 2120-2130.
- G. J. P. Britovsek, S. Mastroianni, G. A. Solan, S. P. D. Baugh, C. Redshaw, V. C. Gibson, A. J. P. White, D. J. Williams, M. R. J. Elsegood, *Chem.-Eur. J.*, **2000**, *6*, 2221-2231. B. L. Small, M. Brookhart, A. M. A. Bennett, *J. Am. Chem. Soc.*, **1998**, *120*, 4049-4050. B. L. Small, M. Brookhart, *J. Am. Chem. Soc.*, **1998**, *120*, 7143-7144. S. C. Bart, E. Lobkovsky, P. J. Chirik, *J. Am. Chem. Soc.* **2004**, *126*, 13794-13807. J. Scott, I. Vidyaratne, I. Korobkov, S. Gambarotta, P. H. M. Budzelaar, *Inorg. Chem.* **2008**, *47*, 896-911.
- R. A. Begum, D. Powell, and K. Bowman-James: *Inorg. Chem.* **2006**, *45*, 964. M. A. Hossain, S. Lucarini, D. Powell, and K. Bowman-James: *Inorg. Chem.* **2004**, *43*, 7275-7277. T. Kanbara, K. Okada, T. Yamamoto, H. Ogawa and T. Inoue: *J. Organomet. Chem.* **2004**, *689*, 1860. K. Okamoto, T. Yamamoto, M. Akita, A. Wada, and T. Kanbara: *Organometallics* **2009**, *28*, 3307-3310.
- T. Teratani, T. Koizumi, T. Yamamoto, K. Tanaka, T. Kanbara *Dalton Trans.*, **2011**, *40*, 8879-8886.
- L. E. Karagiannidis, P. A. Gale, M. E. Light, M. Massi and M. I. Ogden: *Dalton Trans.* **2011**, *40*, 12097-12105. G. W. Bates, P. A. Gale, M. E. Light, M. I. Ogden, C. N. Warriner, *Dalton Trans.*, **2008**, 4106-4112.
- M. Ray, D. Ghosh, Z. Shirin, and R. Mukherjee: *Inorg. Chem.* **1997**, *36*, 3568-3572.
- P. V. Bernhardt, P. C. Sharpe, M. Islam, D. B. Lovejoy, D. S. Kalinowski, D. R. Richardson, *J. Med. Chem.* **2009**, *52*, 407-415. D. R. Richardson, D. S. Kalinowski, V. Richardson, P. C. Sharpe, D. B. Lovejoy, M. Islam, P. V. Bernhardt, *J. Med. Chem.* **2009**, *52*, 1459-1470. D. S. Kalinowski, P. C. Sharpe, P. V. Bernhardt, D. R. Richardson, *J. Med. Chem.* **2007**, *50*, 6212-6225.
- A. W. Addison T. N. Rao, J. Reedijk, J. van Rijn, G. C. Verschoor *J. Chem. Soc. Dalton Trans.* **1984**, 1349-1356.
- Jie Xiao, Liang Deng *Organometallics*, **2012**, *31*, 428-434.
- G. J. P. Britovsek, M. Bruce, V. C. Gibson, B. S. Kimberley, P. J. Maddox, S. Mastroianni, S. J. McTavish, C. Redshaw, G. A. Solan, S. Strömberg, A. J. P. White, D. J. Williams, *J. Am. Chem. Soc.* **1999**, *121*, 8728-8740.
- T. M. Smit, A. K. Tomov, V. C. Gibson, A. J. P. White, D. J. Williams, *Inorg. Chem.* **2004**, *43*, 6511-6512. T. M. Smit, A.K. Tomov, G. J. P. Britovsek, V. C. Gibson, A. J. P. White, D. J. Williams, *Catal. Sci. Technol.*, **2012**, *2*, 643-655.
- G. J. P. Britovsek, V. C. Gibson, B. S. Kimberley, P. J. Maddox, S. J.

ARTICLE

Journal Name

- McTavish, G. A. Solan, A. J. P. White, D. J. Williams, *Chem. Commun.*, **1998**, 849-850.
13. M. W. Bouwkamp, E. Lobkovsky, P. J. Chirik, *Inorg. Chem.* **2006**, *45*, 2-4.
E. C. Weintrob, D. Tofan, J. E. Bercaw, *Inorg. Chem.* **2009**, *48*, 3808-3813.
A. Kayal, S. C. Lee, *Inorg. Chem.* **2002**, *41*, 321-330. R. Çelenligil-Çetin,
P. Paraskevopoulou, R. Dinda, N. Lalioti, Y. Sanakis, A. M. Rawashdeh, R.
J. Staples, E. Sinn, P. Stavropoulos, *Eur. J. Inorg. Chem.* **2008**, 673-677. J.
Xiao, L. Deng *Organometallics*, **2012**, *31*, 428-434.
14. R. G. Pearson, *Survey. Prog. Chem.* **1969**, *5*, 1-52.
15. B. L. An, M. L. Gong, J. M. Zhang, S. L. Zheng, *Polyhedron* **2003**, *22*,
2719 – 2724.
16. A. Altomare, G. Cascarano, C. Giacovazzo, A. Guagliardi, M. C. Burla,
G. Polidori and M. Camalli, *J. Appl. Cryst.*, **1994**, *27*, 435.
17. M. C. Burla, R. Caliandro, M. Camalli, B. Carrozzini, G. L. Cascarano, L.
De Caro, C. Giacovazzo, G. Polidori and R. Spagna, *J. Appl. Cryst.*, **2005**,
38, 381-388.
18. G. Sheldrick, *Acta Cryst. A*, **2008**, *64*, 112-122.
19. D. T. Cromer and J. T. Waber, *International Tables for X-ray
Crystallography*, **1974**.
20. J. A. Ibers and W. C. Hamilton, *Acta Cryst.*, **1964**, *17*, 781-782.
21. D. C. Creagh and W. J. McAuley, *International Tables for
Crystallography*, **1992**, 219-222.
22. D. C. Creagh and J. H. Hubbell, *International Tables for Crystallography*,
1992, 200-206.
23. G. Berthon-Gelloz, M. A. Siegler, A. L. Spek, B. Tinant, J. N. H. Reek, I.
E. Markó *Dalton Trans.* **2010**, *39*, 1444-1446.